Structure of small clusters of parahydrogen molecules

Rafael Guardiola[1] and Jesús Navarro[2]
[1]*Departamento de Física Atómica y Nuclear, Facultad de Física, 46100 Burjassot, Spain*
[2]*Instituto de Fisica Corpuscular, Consejo Superior de Investigaciones Cientificas-Universidad de Valencia, Apdo. 22085, 46071 Valencia, Spain*

(Received 17 February 2006; published 7 August 2006)

The ground state energies and the one-body densities of parahydrogen clusters have been systematically calculated by the diffusion Monte Carlo technique in steps of one molecule from 3 to 50 molecules. These calculations show that parahydrogen clusters exhibit a clear geometrical order which excludes any liquidlike structure. A definite confirmation of the magic size for the cluster with 13 molecules is also obtained.

DOI: 10.1103/PhysRevA.74.025201 PACS number(s): 36.40.−c, 61.46.Bc

At low temperature, parahydrogen molecules (p-H_2) are in the ground state with zero angular momentum, and thus are spinless bosons such as ^{4}He atoms. Although the p-H_2 molecule has a lighter mass than ^{4}He, the van der Waals interaction is much more attractive, and the bulk phase is a hcp solid. The path integral Monte Carlo simulations of Sindzingre *et al.* [1] have shown that at temperatures below $T \simeq 2$ K the superfluid fraction in clusters with 13 and 18 p-H_2 molecules become large. These results have motivated both experimental [2] and theoretical [3–6] research of the rotational spectra of the OCS molecule inside small p-H_2 clusters, analogously to the OCS-^4He_N systems where superfluidity in finite systems was established [7].

In this work we address the question of the structure of pure small p-H_2 clusters at very low temperature. These clusters can be pictured as small pieces of the bulk solid (i.e., a crystalline structure) or as nanodroplets of a liquid or, finally, as clusters with a geometrical ordered noncrystaline structure. In the latter case, magic sizes related to the completion of geometrical shells are to be expected.

In a recent experiment [8] small p-H_2 clusters have been produced in a cryogenic free jet expansion and studied by Raman spectroscopy. It has been observed that the $Q(0)$ Raman line of the H_2 monomer is shifted as the number of molecules in the cluster changes, thus providing a method to determine the cluster mass. The first resolved peaks next the monomer line have been assigned to $(p\text{-}H_2)_N$ clusters with $N=2,\ldots,8$ molecules. The resolution in that experiment was not enough to resolve larger cluster sizes, but broad maxima were observed at $N \approx 13$, 33, and 55. These maxima were considered as magic sizes related to geometric shells. Interestingly, such numbers correspond to the so-called Mackay icosahedra [9], which are expected structures for small classical Lennard-Jones clusters. A very complete discussion of classical geometrical patterns and their relation with the interaction features can be found in Ref. [10].

Quantum Monte Carlo methods have been used in the past to study p-H_2 clusters, namely, variational Monte Carlo (VMC) and diffusion Monte Carlo (DMC) methods [11–13] or path integral Monte Carlo (PIMC) methods [1,14]. In all cases the study has been limited to specific values of the number of constituents N, presumably motivated by the classical static [16–18] or molecular dynamics [18,19] results related to a generic Lennard-Jones interaction potential.

We present in this paper DMC simulations to systematically analyze the energetics and structure of $(p\text{-}H_2)_N$ clusters at $T=0$ with $N=3,\ldots,50$, with the aim of finding signal of magic sizes in this interval and also discern their structure. We have used the isotropic pairwise interaction modelled by Buck *et al.* [20].

The calculations are based on a Jastrow-like importance sampling wave function depending on just two parameters

$$\Phi = \prod_{i<j}^{N} \exp\left(-\frac{1}{2}\left(\frac{r_{ij}}{b}\right)^5 - \frac{r_{ij}}{p}\right), \tag{1}$$

where r_{ij} is the relative coordinate of the pair (i,j). After systematic minimization of the parameters for each value of N it was found that the parameter b controlling the short-range part of the correlations is practically constant, with the value $b=3.70$ Å. On the other hand, the long-range parameter p varies almost linearly, from 2.24 Å for $N=3$ up to 23.6 Å for $N=50$. Afterwads, the DMC calculations were carried out with very small real-time steps (5×10^{-5} to 1×10^{-5} K^{-1}, for the light and heavier clusters, respectively) and very long number of evaluation steps. Notice that the Bose symmetry of the above guiding wave function is not modified in the DMC process.

The calculated DMC ground state energies are displayed in Table I. Special care was taken to estimate the statistical error: the raw results were analyzed by averaging in blocks of increasing number of successive time steps until the standard deviation became stable, thus removing the unavoidable correlations inherent to the short-step stochastic evolution. The numbers given in parenthesis in the table are the errors in the final digit shown. Our results agree, as they should, with previous calculations employing the same interaction. For instance, the DMC energies per molecule obtained in Ref. [13] are −12.1649(7), −14.13(2), −22.85(7), and −35.12(6), respectively for $N=6$, 7, 13, and 33. Although the trial wave function used in Ref. [13] contains nine parameters, our simpler wave function leads to similar VMC values and, after a long enough simulation run, to compatible DMC energies. There is also a qualitative agreement with the extrapolation to zero temperature of the PIMC results of Ref. [1], based on the same intermolecular interaction, as well as the PIMC results of Ref. [14], which used instead the Silvera-Goldman interaction [15].

The total binding energies grow monotonically with the number of constituents. In order to determine an enhanced

TABLE I. Ground state $(p\text{-}H_2)_N$ energies per molecule $E(N)/N$ (in K) obtained in a DMC calculation. The statistical standard deviation is indicated in parenthesis (error in the final digit shown).

N	$-E(N)/N$	N	$-E(N)/N$	N	$-E(N)/N$
3	4.893(7)	19	27.78(2)	35	36.13(2)
4	7.618(8)	20	28.44(2)	36	36.44(2)
5	10.09(1)	21	29.13(2)	37	36.81(2)
6	12.24(1)	22	29.77(2)	38	37.10(2)
7	14.12(1)	23	29.94(2)	39	37.41(2)
8	15.78(1)	24	31.03(2)	40	37.72(2)
9	17.29(1)	25	31.64(2)	41	38.05(2)
10	18.69(2)	26	32.22(2)	42	38.34(2)
11	20.14(1)	27	32.76(2)	43	38.58(2)
12	21.65(2)	28	33.23(2)	44	38.92(2)
13	22.99(3)	29	33.73(2)	45	39.22(2)
14	23.99(2)	30	34.12(2)	46	39.56(2)
15	24.84(2)	31	34.60(2)	47	39.78(2)
16	25.62(2)	32	35.01(2)	48	40.08(3)
17	26.31(2)	33	35.41(2)	49	40.36(4)
18	27.01(2)	34	35.76(2)	50	40.61(4)

stability related to magic sizes it is convenient to analyze the variation with N of the dissociation energy or chemical potential, defined from the ground state energies $E(N)$ as

$$\mu_N = E(N-1) - E(N). \tag{2}$$

This quantity is plotted in Fig. 1. The most appealing feature of this plot is the presence of a bump around $N=13$; the bump starts at $N=10$, with a clear change of the slope, reaches its maximum at $N=13$ and afterwards there is a sudden drop followed by a plateau until $N=17$. This indicates that $N=13$ is a true magic cluster, in agreement with the experimental findings of Ref. [8].

Afterwards there is no clear signal of any local enhancement of the chemical potential. It should be mentioned that even if the sampling has been pursued until the standard deviation of the energy per particle remains constant, near 0.02 K, when subtracting the total energies to obtain the chemical potential the corresponding standard deviation grows monotonically thus hiding possible minor local structures. So, the only local irregularities (near 30 and 40 constituents) cannot be properly considered as real bumps, and consequently as real magical numbers.

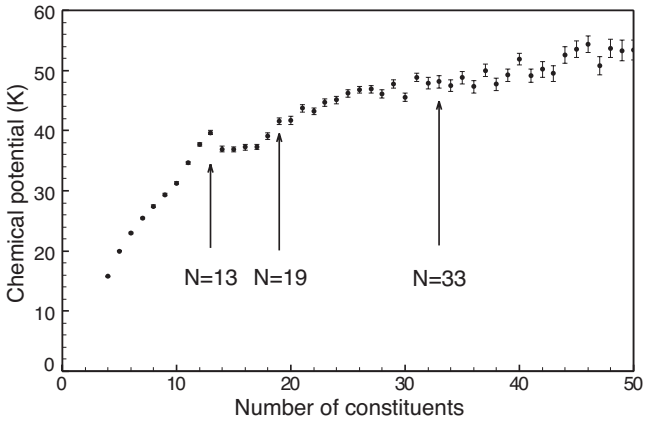

FIG. 1. DMC chemical potential (in K) of $(p\text{-}H_2)_N$ clusters as a function of the number N of constituents.

The other question of relevance for $p\text{-}H_2$ clusters is their shape. It is convenient to consider briefly the corresponding results from classical simulations. From the static point of view the potential energy surfaces have an enormously large number of local minima. In fact, it has been stated [22] that determining the ground state of a cluster of identical atoms interacting under two-body central forces belongs to the class of Np-hard problems, meaning that no polynomial time algorithm solving this problem exists. For the $N=13$ problem Hoare and McInnes [23] found 988 local minima. Honeycutt and Andersen [18] heated and cooled the molecular dynamics evolution to find the most favorable patterns at $T=0$, and from their results (not covering all clusters) it is interesting to mention that for $N=13$ and $N=55$ they found a quite large energy gap between the absolute minimum and the next geometrical arrangement, both minima corresponding to icosahedral shapes, as well as a less pronounced gap at $N=19$ (double icosahedron). These results correspond to Lennard-Jones systems.

Previous quantum determinations have tried to get some parallelism with classical clusters, by analyzing instantaneous snapshots along the stochastic random walk. In this manner it has been found that from time to time specific clusters do adopt geometrical shapes with pentagonal symmetry. Thus, $N=13$ is pictured as a body-centered icosahedron (12 particles, one at each vertex, plus one in the center-of-mass); $N=19$ is pictured as four single particles in the symmetry axis alternating with three parallel pentagons; finally, $N=34$ shows a 7 particle core (bipyramidal pentagonal) plus 27 particles distributed in two close spherical shells, with clear pentagonal symmetry. The reader may consult Refs. [10,14] to find drawings of these configurations.

Whereas this classical-like analysis may be done for a few specific clusters, it will be cumbersome for a large number of clusters. We have preferred instead to consider just the one-body density distribution given by the expectation value

$$\rho(\mathbf{r}) = \sum_{i=1}^{N} \langle \delta(\mathbf{r} - (\mathbf{r}_i - \mathbf{R})) \rangle, \tag{3}$$

where $\mathbf{r}_i$ stands for the ith-particle coordinates, and $\mathbf{R} = \Sigma_i \mathbf{r}_i / N$ is the center-of-mass of the system. Given that the clusters have zero angular momentum, the outcoming one-body density is spherically symmetric, within statistical fluctuations.

The density distributions, normalized to the number of constituents, are represented in Fig. 2, for $N=3$ to 50. There is a clear evolution of the density distributions with the number of constituents: hydrogen molecules are arranged in quite sharply defined spherical shells, with radii growing slowly but steadily with the number of molecules. There are two

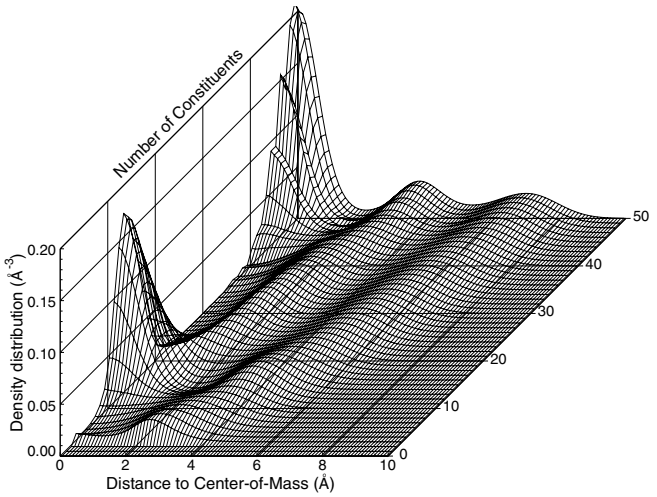

FIG. 2. The density distribution of $(p\text{-}H_2)_N$ clusters as a function of the number N of constituents, obtained by the DMC method. Distances are measured in Å and densities correspond to the number of molecules per cubic Å.

regions, around $N=13$ and 50 with a very large peak near the center-of-mass, and in the middle region the space near the center of mass is empty. It should be mentioned that these two features do not appear in the densities obtained with the optimized VMC trial functions, so that they are developed along the DMC real-time evolution. This fact was also found in the calculations of McMahon and Whaley [13] for clusters with $N=6$, 13, and 33.

In order to ascertain the location of the second maximum at the origin we have pushed our calculations up to $N=70$. The calculations clearly show that the peak of the density at the origin grows up to $N=55$, and afterwards drops to zero around $N=70$. The structure pattern near $N=55$ is similar to the one observed around $N=13$. Due to the smaller statistics in the calculations for $N>50$, the calculated binding energies are affected by a rather large statistical error. We have thus preferred to limit the values displayed in Table I and Fig. 1 to the maximum value $N=50$.

Just from Fig. 1 one may conclude that the small p-H_2 clusters cannot be considered as small droplets. Actually, it is very instructive to compare the present density distributions with those obtained for the ^{4}He nanodroplets [21]. The latter are rather constant in the inner volume, as expected for a liquid drop, presenting only slight oscillations at the surface.

In order to get a more precise description of the shells appearing in the density distributions, it is useful to resolve them in terms of overlapping Gaussians,

$$\rho(r) \approx \sum_k A_k \exp\left(-\frac{(r-c_k)^2}{2\sigma_k^2}\right), \tag{4}$$

where the number of terms of the sum depends of the shape of the distribution. In each term, the centroid c_k signals the region where the density has a local maximum and the width σ_k is a measure of how sharp this region is defined.

By integrating the individual Gaussians one may determine the number of particles lying in the corresponding shell. The results are presented in Fig. 3, where the number of particles has been rounded to the nearest integer. Notice that in some cases, the existence of important overlaps between the Gaussians can create some conflict in the number of particles assigned to each shell.

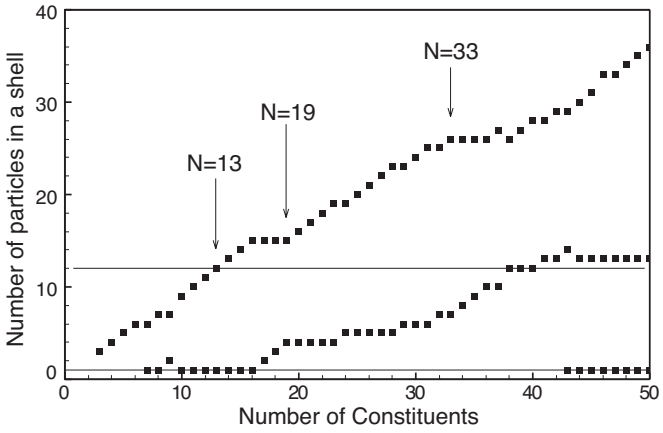

FIG. 3. The number of particles ascribed to each shell as a function of the number of constituents of the cluster. The horizontal lines correspond to 1 and 12 particles.

A quite surprising feature emerging from the Gaussian resolution is that the regions with a very large value of the density near the center of mass do actually have a single particle. Moreover, from $N=20$ and beyond there are two shells which are simultaneously filled as the size of the cluster increases. In conclusion, we have observed structural changes around $N=13$ and 55 (maximum density at the origin) and no special signal at $N=33$.

The occupation numbers obtained here are basically in agreement with previous findings based on snapshots of the molecules in a cluster. For example, our calculated distribution for $N=13$ agrees with the geometrical picture of one particle in the center and 12 particles in the vertices of an icosahedron. For $N=33$ the occupation numbers are compatible with a double pentagonal pyramid (7 particles) near the center, and the remaining 26 particles in an external shell. However, our density profiles are less structured than those found by Scharf *et al.* [14] in their PIMC calculation at 2.5 K. Actually, for $N=33$ and 34 we just find two broad peaks at around 2.5 and 6 Å, instead of the two double peaks displayed in Fig. 6 of Ref. [14]. We believe this differences may be a consequence of the excited states admixture associated with the PIMC algortihm.

In conclusion, our DMC calculations at zero temperature show that $(p\text{-}H_2)_N$ clusters exhibit a clear geometrical order, with the molecules distributed in spherical coronas. A significant Bose condensed fraction was found in the PIMC simulations of Ref. [1] for clusters with 13 and 18 molecules. That result was confirmed by the experiments of Ref. [2]. As the present DMC calculations excludes a standard liquid-like structure, an intriguing question is open regarding the behavior of p-H_2 molecules inside the spherical coronas: they could either move as in a liquid or, on the contrary, they could be tied to some fixed positions as in a Mackay icosahedron.

With respect to magical numbers, there is a definite confirmation of $N=13$. From the present calculations we cannot definitely conclude about the nature of $N\approx 33$ hydrogen clusters; in our opinion, $N=33$ is not a magical cluster, because from the structure near $N=13$ we should expect a region of enhanced stability, if it were magical, instead of a single spike. To this respect it is worth mentioning that magic sizes have also been observed in ^{4}He clusters [24], which are definitely liquidlike and thus the magic sizes are not related to enhanced ground state binding energies at specific values of N. They are instead stability thresholds, related to the cluster sizes at which excited levels cross the chemical potential curve and become stabilized. An analysis of the possible existence of similar stability thresholds in p-H_2 could be helpful to interpret the experimental results of Ref. [8].

Stimulating discussions with O. Kornilov, J.P. Toennies, and S. Montero are gratefully acknowledged. This work was supported by MCyT (Spain), Grant No. FIS2004-0912.

[1] Ph. Sindzingre, D. M. Ceperley, and M. L. Klein, Phys. Rev. Lett. **67**, 1871 (1991).
[2] S. Grebenev, B. Sartakov, J. P. Toennies, and A. F. Vilesov, Science **289**, 1532 (2000).
[3] Y. Kwon and K. B. Whaley, Phys. Rev. Lett. **89**, 273401 (2002).
[4] F. Paesani, R. E. Zillich, and K. B. Whaley, J. Chem. Phys. **119**, 11682 (2003).
[5] J. Tang and A. R. W. McKellar, J. Chem. Phys. **121**, 3087 (2004).
[6] F. Paesani, R. E. Zillich, Y. Kown, and K. B. Whaley, J. Chem. Phys. **122**, 181106 (2005).
[7] S. Grebenev, J. P. Toennies, and A. F. Vilesov, Science **279**, 2083 (1998).
[8] G. Tejeda, J. M. Fernández, S. Montero, D. Blume, and J. P. Toennies, Phys. Rev. Lett. **92**, 223401 (2004).
[9] A. L. Mackay, J. Appl. Crystallogr. **15**, 916 (1962).
[10] F. Baletto and R. Ferrando, Rev. Mod. Phys. **77**, 317 (2005).
[11] M. V. Rama Krishna and K. B. Whaley, Z. Phys. D: At., Mol. Clusters **20**, 223 (1991).
[12] M. A. McMahon, R. N. Barnett, and K. B. Whaley, J. Chem. Phys. **99**, 8818 (1993).
[13] M. A. McMahon and K. B. Whaley, Chem. Phys. **182**, 119 (1994).
[14] D. Scharf, M. L. Klein, and G. J. Martyna, J. Chem. Phys. **97**, 3590 (1992).
[15] I. F. Silvera and V. V. Goldman, J. Chem. Phys. **69**, 4209 (1978).
[16] M. R. Hoare and P. Pal, Adv. Phys. **20**, 161 (1971).
[17] M. R. Hoare, Adv. Chem. Phys. **40**, 49 (1979).
[18] J. D. Honeycutt and H. C. Andersen, J. Phys. Chem. **91**, 4950 (1987).
[19] J. Jellinek, T. L. Beck, and R. S. Berry, J. Chem. Phys. **84**, 2783 (1986).
[20] U. Buck, F. Huisken, A. Kohlhase, D. Otten, and J. Schaeffer, J. Chem. Phys. **78**, 4439 (1983).
[21] R. Guardiola, O. Kornilov, J. Navarro., and J. P. Toennies, J. Chem. Phys. **124**, 084307 (2006).
[22] L. T. Wille and J. Vennik, J. Phys. A **18**, L419 (1985).
[23] M. R. Hoare and J. McInnes, J. Chem. Soc., Faraday Trans. 1 **61**, 12 (1976).
[24] R. Brühl, R. Guardiola, A. Kalinin, O. Kornilov, J. Navarro, T. Savas, and J. P. Toennies, Phys. Rev. Lett. **92**, 185301 (2004).